

EVALUATION OF NANOSTRUCTURED BOND COAT IN THERMAL
BARRIER COATING SYSTEM WITH NANO ALUMINA LAYER DURING
OXIDATION

MOHAMMADREZA DAROONPARVAR

A thesis submitted in fulfillment of the
requirements for the award of the degree of
Doctor of Philosophy (Mechanical Engineering)

Faculty of Mechanical Engineering
Universiti Teknologi Malaysia

JUNE 2013

To my beloved parents and wife thanks for all your affectionate caring and supporting, and above all your sacrifices and prayers accorded to me until the successful completion of this project.

“My Success Is Yours Too”

ACKNOWLEDGEMENT

In preparing this thesis, I was in contact with many people, researchers, academicians, and practitioners. They have contributed towards my understanding and thoughts. In particular, I wish to express my sincere appreciation to my thesis supervisors, Dr. Muhamad Azizi Mat Yajid and Professor. Dr. Noordin Mohd Yusof for encouragement, guidance, critics and friendship. I am also very thankful to all members in department of materials, manufacturing and industrial engineering for their useful guidance related to materials engineering matters. I also extended my sincere gratitude to all the materials laboratory's technicians for helping me to carry out all the tests throughout my studies.

I am also indebted to Universiti Teknologi Malaysia (UTM) for funding my Ph.D. study. My sincere appreciation also extends to all my colleagues and others who have provided assistance at various occasions. Their views and tips are useful indeed. Unfortunately, it is not possible to list all of them in this limited space. I am grateful to all my family members.

ABSTRACT

A thermal barrier coating (TBC) system usually consists of a ceramic top coat (yttria stabilized zirconia or YSZ) and a metallic bond coat (MCrAlY) (M = Ni, Co or mixture of these two) on the nickel-based superalloy as a substrate. A thermally grown oxide (TGO) layer can be easily formed on the bond coat which plays an important role in the spallation of TBC due to its growth during oxidation. Hence, the principal purpose of this research is to provide a new coating to significantly lessen the TGO growth and to suppress the growth of detrimental mixed oxides (CSNs) on the Al_2O_3 (TGO) layer during oxidation. Therefore, air plasma sprayed normal and nano TBC systems including, Inconel 738/normal NiCrAlY/normal YSZ, Inconel 738/normal NiCrAlY/normal YSZ/normal Al_2O_3 , Inconel 738/nano NiCrAlY/normal YSZ, Inconel 738/nano NiCrAlY/normal YSZ/nano Al_2O_3 (as a novel system), and Inconel 738/normal NiCrAlY/nano YSZ were prepared then evaluated by pre-oxidation at 1000°C for 48h, high temperature oxidation at 1000°C for 120h, cyclic oxidation (thermal shocks) at 1150°C and finally hot corrosion test at 1000°C. Microstructural characterization of coatings was also performed using SEM, FESEM, XRD and EDX. The results showed that both TGO growth and CSNs were considerably reduced with the use of nano NiCrAlY/YSZ/nano Al_2O_3 coating compared to the other coatings. It was found that pre-oxidation treatment and particularly TBC system microstructure can influence the evolution of TGO layer and TBCs durability during service at elevated temperatures.

ABSTRAK

Sistem salutan halangan haba (TBC) biasanya mengandungi satu lapisan seramik sebagai lapisan atas (YSZ atau yttria distabilkan zirconia) dan satu lapisan logam sebagai lapisan pengikat (MCrAlY) (M = Ni, Co atau campuran keduanya) di atas substrat superaloi berasaskan nikel. Satu lapisan oksida tertumbuh haba (TGO) akan terbentuk dengan mudah di atas lapisan pengikat yang memainkan peranan yang penting dalam proses serpihan TBC yang disebabkan oleh pertumbuhan lapisan TGO semasa pengoksidaan. Jadi, tujuan utama penyelidikan ini adalah untuk membentuk satu salutan baru untuk mengurangkan kadar pertumbuhan lapisan TGO dan mengurangkan dengan berkesan pembentukan campuran oksida yang merosakkan (CSNs) di atas lapisan Al_2O_3 (TGO) semasa pengoksidaan. Oleh itu, beberapa sistem TBC iaitu normal dan nano disediakan melalui kaedah semburan plasma iaitu Inconel 738/normal NiCrAlY/normal YSZ, Inconel 738/normal NiCrAlY/normal YSZ/ normal Al_2O_3 , Inconel 738/nano NiCrAlY/ normal YSZ, Inconel 738/nano NiCrAlY/normal YSZ/nano Al_2O_3 (sistem *novel*) dan Inconel 738/normal NiCrAlY/nano YSZ yang kemudiannya dinilai melalui kaedah pra-pengoksidaan pada suhu 1000°C selama 48 jam, pengoksidaan pada suhu tinggi pada suhu 1000°C selama 120 jam, pengoksidaan berkitar (kejutan suhu) pada suhu 1150°C dan seterusnya ujian kakisan panas pada suhu 1000°C . Pencirian mikrostruktur terhadap salutan yang terbentuk telah dilakukan melalui beberapa kaedah SEM, FESEM, XRD dan EDX. Keputusan kajian ini mendapati kedua-dua pertumbuhan TGO dan CSN telah berkurangan dengan begitu ketara bagi salutan nano NiCrAlY/YSZ/nano Al_2O_3 , berbanding dengan salutan-salutan lain. Didapati juga, mikrostruktur dari rawatan pra-pengoksidaan terutamanya sistem TBC yang digunakan boleh mempengaruhi evolusi pembentukan lapisan TGO dan kebolehtahanan sistem salutan semasa digunakan pada suhu tinggi.

TABLE OF CONTENTS

CHAPTER	TITLE	PAGE
	DECLARATION	ii
	DEDICATIONS	iii
	ACKNOWLEDGEMENTS	iv
	ABSTRACT	v
	ABSTRAK	vi
	TABLE OF CONTENTS	vii
	LIST OF TABLES	xv
	LIST OF FIGURES	xvi
	LIST OF ABBREVIATIONS	xxxii
	LIST OF APPENDICES	xxxiii
1	INTRODUCTION	1
	1.1 Research Background	1
	1.2 Problem Statement	3
	1.3 Purpose of the Study	5
	1.4 Objectives of the Study	7
	1.5 Scopes of Work	7
	1.6 Organization of Thesis	9
2	LITERATURE REVIEW	11
	2.1 Introduction of Thermal Barrier Coating Systems	11
	2.1.1 MCrAlY as Bond Coat in TBCs (Thermal Barrier Coating Systems)	13
	2.1.2 YSZ as Top Coat in TBCs	14
	2.1.2.1 Phase Transformation of Pure	14

	Zirconia at Elevated Temperatures	
2.1.2.2	Alloying of Zirconia with the other Stable Oxides	14
2.2	Oxidation as Principal Problem of TBCs at Elevated Temperatures	16
2.2.1	Detrimental Mixed Oxides Formation and Growth on the Al_2O_3 Oxide Scale During Oxidation	22
2.3	Methods Which Can Reduce Oxidation of TBC Systems	27
2.3.1	Micro-Structured Al_2O_3 as a Third Layer in TBC systems	27
2.3.2	Nanostructured NiCrAlY Layer as Bond Coat in TBC Systems	29
2.3.3	Nanostructured YSZ Layer as Top Coat in TBC Systems	33
2.4	Hot Corrosion Phenomenon in Thermal Barrier Coatings	35
2.5	Microstructural Investigation of Plasma Sprayed Coatings	43
2.6	The Oxidation kinetic of the Bond Coat in TBC Systems	45
2.7	The Other Important Research Activities for Modifying the Properties of TBCs at Elevated Temperatures	46
2.7.1	Utilizing Ceramic Layer of $\text{ZrO}_2 - \text{CeO}_2 - \text{Y}_2\text{O}_3$ as Top Coat	46
2.7.2	FGM coatings	46
2.7.3	Improvement of TBCs Properties using Laser Treatment	48
2.7.4	LPHS Method	49
2.8	Comparison of Alumina (Al_2O_3) and Zirconia (YSZ) Properties in TBCs	49

3	METHODOLOGY	52
3.1	Introduction	52
3.2	Characteristics of Feed Stokes (Ni-Based Superalloy as Base Metal and as-Received Powders)	54
3.2.1	Ni-Based Superalloy (Inconel 738) as a Base Metal	54
3.2.2	As-Received Powders	54
3.2.2.1	Normal NiCrAlY Powders (AMDRY 962 POWDER)	54
3.2.2.2	Normal YSZ (8% Yittria Stabilized Zirconia) Powders as TBC	55
3.2.2.3	Nano Al ₂ O ₃ Powders	55
3.2.2.4	Normal Al ₂ O ₃ Powders	55
3.2.2.5	Granulated Nano YSZ Powders	56
3.3	The Preparation of as-Received Powders for Air Plasma Spraying	56
3.3.1	Granulation of Nano Al ₂ O ₃ Powders	56
3.3.2	The Preparation of Nano NiCrAlY Powders Using a Planetary Ball Mill Device	57
3.3.3	The Preparation of Substrates (Inconel 738) Surface for Air Plasma Spraying (APS)	59
3.4	Deposition of Coatings on the Base Metal (Inconel 738) using Air Plasma Spraying Method	61
3.4.1	Air Plasma Spraying (APS) Method	61
3.5	Introduction of Air Plasma Sprayed Coatings	64
3.5.1	Normal TBC System (Inconel 738/Normal NiCrAlY/Normal YSZ)	64
3.5.2	Nano TBC System (Inconel 738 / Nano NiCrAlY / Normal YSZ)	65
3.5.3	Triple layered Normal TBC System (Inconel 738/Normal NiCrAlY/Normal YSZ/Normal Al ₂ O ₃)	65
3.5.4	Triple layered Nano TBC System (Inconel	66

	738/Nano NiCrAlY/Normal YSZ/Nano Al ₂ O ₃)	
	3.5.5 Nano TBC System with Nanostructured YSZ (Inconel 738/Normal NiCrAlY/Nano YSZ)	67
3.6	Investigation of As-Sprayed Coatings	67
3.6.1	Isothermal Pre -Oxidation Test at 1000°C and Cyclic Oxidation (Thermal Shocks) Test at 1150°C	67
3.6.2	High Temperature Oxidation Resistance of As- Sprayed TBCs at 1000°C	68
3.6.3	Hot Corrosion Resistance Test at 1000°C	68
3.7	Microstructural Characterization using SEM and FESEM Equipped With EDS	70
3.7.1	Morphology Investigation of As-Received Powders and Microstructural Investigation of As-Sprayed TBCs	70
3.7.1.1	Microstructural Characterization of As-Sprayed TBCs	72
3.7.2	Morphological Investigation of NiCrAlY Powders after Milling Process	72
3.7.3	Microstructural Investigation of TBC Systems after Oxidation Tests	72
3.7.4	Microstructural Characterization of TBCs after Hot Corrosion Test	73
3.8	Phase Analysis using XRD	73
3.8.1	Phase Analysis of Outer Surface of As-Sprayed TBCs, As-Received, Granulated and Milled Powders using XRD	73
3.8.2	Phase Analysis after Isothermal and Cyclic Oxidation Tests	75
3.8.3	Phase Analysis after Hot Corrosion Test	75
4	RESULTS AND DISCUSSION	76
4.1	The Characterization of Prepared Powders and As-	76

Sprayed Coatings	
4.1.1 Introduction	76
4.1.2 Microstructural Characterization of NiCrAlY Powders before and after Milling Process	77
4.1.3 Microstructural Characterization of Granulated Nano Al ₂ O ₃ Powders	80
4.1.4 Microstructural Characterization of used Corrosive Salts for Hot Corrosion Test	82
4.1.5 Microstructural Characterization of Air Plasma Sprayed Coatings	84
4.1.5.1 Normal Thermal Barrier Coating system (Normal NiCrAlY / Normal YSZ)	84
4.1.5.2 Nano Thermal Barrier Coating System (Inconel 738/Nano NiCrAlY/ Normal YSZ)	89
4.1.5.3 The Triple Layered Normal Thermal Barrier Coating System (Inconel 738/Normal NiCrAlY / Normal YSZ / Normal Al ₂ O ₃)	92
4.1.5.4 The Triple Layered Nano Thermal Barrier Coating System (Inconel 738/ Nano NiCrAlY / Normal YSZ / Nano Al ₂ O ₃)	97
4.1.5.5 Nano Thermal Barrier Coating System with Nanostructured YSZ (Inconel 738/ Normal NiCrAlY / Nano YSZ)	101
4.1.6 Summary	107
4.2 Improvement of Thermally Grown Oxide Layer in Thermal Barrier Coating Systems with Nano Alumina as a Third Layer During Isothermal Oxidation	108
4.2.1 Introduction	108

4.2.2	The Microstructural Characterization of TBCs After Isothermal Oxidation at 1000°C	108
4.2.3	Summary	122
4.3	Investigation of Hot Corrosion Resistance of YSZ/nano Al ₂ O ₃ Coating at 1000 °C	124
4.3.1	Introduction	124
4.3.2	Microstructural Characterization of Coatings after Hot Corrosion Test	124
4.3.3	Hot Corrosion Mechanism of YSZ Coating at Elevated Temperatures	131
4.3.4	Summary	136
4.4	The Role of Formation of Continuous Thermally Grown Oxide Layer on the Nanostructured NiCrAlY Bond Coat during Thermal Exposure (Pre-Oxidation + Cyclic Oxidation) in Air	138
4.4.1	Introduction	138
4.4.2	Microstructural Characterization of TBCs after Pre-Oxidation Test at 1000°C	138
4.4.3	The Microstructural Characterization of Pre-oxidized TBCs after Cyclic Oxidation Test at 1150°C	141
4.4.4	Summary	149
4.5	Formation of a Thinner and Continuous Al ₂ O ₃ Layer in Nano Thermal Barrier Coating Systems for the Suppression of Spinel Growth on the Al ₂ O ₃ Oxide Scale during Cyclic Oxidation	151
4.5.1	Introduction	151
4.5.2	Microstructural Characterization of different Thermal Barrier Coating Systems after Isothermal Pre-Oxidation Test At 1000°C	151
4.5.3	The Microstructural Characterization of Pre-oxidized Thermal Barrier Coating Systems after Cyclic Oxidation Test at 1150°C	156

4.5.4	Summary	170
4.6	The High Temperature Oxidation and Corrosion Behavior of Thermal Barrier Coating Systems with Nanostructured YSZ	172
4.6.1	Introduction	172
4.6.2	Hot Corrosion Behavior of Micro-Structured and Nanostructured YSZ Coatings at 1000°C	172
4.6.3	The High Temperature Oxidation Behavior of TBCs at 1000°C	180
4.6.4	Summary	192
4.7	The Formation and Effect of Nearly Continuous but Thinner Thermally Grown Oxide Scale in NiCrAlY/Nanostructured YSZ Coating during Oxidation (Pre-Oxidation + Cyclic Oxidation) Test	194
4.7.1	Introduction	194
4.7.2	Microstructural Investigation of TBC Systems with Micro-structured and Nano-structured YSZ Coatings after Isothermal Pre-Oxidation Test at 1000°C	194
4.7.3	Microstructural Characterization of Pre-Oxidized Thermal Barrier Coating Systems with Micro-structured and Nano-structured YSZ Coatings after Cyclic Oxidation Test at 1150°C	202
4.7.4	Summary	215
5	CONCLUSIONS AND RECOMMENDATION FOR THE FUTURE WORKS	217
5.1	Conclusions	217
5.2	Recommendation for the Future Works	219
	REFERENCES	220

LIST OF TABLES

TABLE NO	TITLE	PAGE
2.1	Comparison of thermal expansion coefficient of Al ₂ O ₃ and ZrO ₂ particles at different temperatures	50
2.2	Thermal conductivity of Al ₂ O ₃ and ZrO ₂ particles at different temperatures	50
3.1	Chemical composition of Inconel 738	54
3.2	Chemical composition of NiCrAlY powders (AMDRY 962)	54
3.3	Chemical composition of normal YSZ powders	55
3.4	Chemical composition of nano Al ₂ O ₃ powders	55
3.5	Chemical composition of normal Al ₂ O ₃ powders	55
3.6	Chemical composition of nano YSZ powders	56
3.7	The parameters of APS method	64
3.8	The physical properties of corrosive materials	69
4.1	The apparent density and flowability of nano Al ₂ O ₃ powders before and after granulation treatment	81
4.2	Hot corrosion test results	173

LIST OF FIGURES

FIGURE NO	TITLE	PAGE
1.1	Schematic illustration of a normal thermal barrier coating system in addition to thermally grown oxide (TGO) layer. The temperature gradient during engine operation can be also observed	4
1.2	Schematic illustration of cross section of air plasma sprayed nano NiCrAlY/normal YSZ/nano Al ₂ O ₃ coating on the Ni-based superalloy (as a novel TBC system) in this research.	8
2.1	Turbine temperatures progression from 1950 to 2010	12
2.2	Cross section of air plasma sprayed normal TBC system	13
2.3	Phase transformation of pure zirconia at different temperatures	14
2.4	Phase diagram of Y ₂ O ₃ - ZrO ₂	16
2.5	Predicted dependence on temperature of the oxygen fluxes for gas permeation and diffusion through a 250 ± 50 μm thick zirconia top coat (TC), representing a maximum pressure and concentration gradient	18
2.6	Deterioration mechanism of TC during oxidation	19
2.7	Internal oxidation of the bond coat at elevated temperatures	20
2.8	TGO layer at the BC/YSZ interface after high temperature oxidation at 1100°C for 100 h	21
2.9	Detrimental mixed oxides at the Al ₂ O ₃ /YSZ interface in APS TBC system (Inconel/normal MCrAlY/normal YSZ); a) granular NiO b) (Cr,Al) ₂ O ₃ (chromia),	23

	(Ni(Cr, Al) ₂ O ₄) (spinel (CS))	
2.10	Radial stress S _x distribution in TBC system with TGO involving a) Al ₂ O ₃ (mono-layered TGO) b) spinel and Al ₂ O ₃ (bi-layered TGO); and axial stress S _y distribution in TBC system with TGO containing c) Al ₂ O ₃ d) spinel and Al ₂ O ₃	24
2.11	APS normal TBC system with normal NiCrAlY as BC a) somewhat continues and thinner Al ₂ O ₃ (TGO) layer formation b) Ni(Cr,Al) ₂ O ₄ ·NiO formation between the Al ₂ O ₃ layer and the YSZ as top coat in some regions after 24 h at 1080 °C in low-pressure oxygen environment	25
2.12	Bi-layered TGO formed in normal TBC system a) after 194 h at 1010°C (spinels formation) b) after 216 h at 1150°C (micro-cracks formation at the Al ₂ O ₃ / YSZ interface or CSNs)	26
2.13	Cross section of normal TBC system with normal Al ₂ O ₃ as a third layer after spraying	28
2.14	TGO thickness versus oxidation time for normal YSZ and normal YSZ/nomal Al ₂ O ₃ coatings after 100h of isothermal oxidation test	28
2.15	TGO layer formation in TBC systems; a) TGO layer formation on the normal NiCrAlY coating b) Formation of TGO layer (nearly continues but thinner) on the nanostructured NiCrAlY coating after high temperature oxidation at 1000°C for 24 h	31
2.16	As-sprayed nano YSZ coating surface	33
2.17	a) Nano YSZ powders b) Nano regions in the as-sprayed nano YSZ coating	34
2.18	Surface of YSZ layer after spallation: monoclinic ZrO ₂ and YVO ₄ crystals as disruptive phases can be observed after hot corrosion test	36
2.19	YVO ₄ small rod crystals with low number on YSZ as inner layer of YSZ/normal Al ₂ O ₃ coating after hot	37

	corrosion test. Normal alumina layer spalled at the YSZ/normal Al ₂ O ₃ interface	
2.20	Cross-section of TBCs after hot corrosion test; a) normal YSZ coating with wide crack at the BC/YSZ interface due to YVO ₄ crystals and monoclinic ZrO ₂ formation b) YSZ/normal Al ₂ O ₃ coating after spallation of normal Al ₂ O ₃ layer	37
2.21	Surface of TBCs after hot corrosion test; a) normal YSZ layer surface with high amount of hot corrosion products b) Gd ₂ Zr ₂ O ₇ + YSZ surface with low amount of hot corrosion products c) Gd ₂ Zr ₂ O ₇ surface with medium amount of hot corrosion products after hot corrosion test in Na ₂ SO ₄ + V ₂ O ₅ at 1050 °C	38
2.22	Morphology of plasma spray-able nano Y ₂ SiO ₅ powders; a) granulated nano Y ₂ SiO ₅ powders b) nano Y ₂ SiO ₅ particles in a granulated particle	40
2.23	Monoclinic zirconia volume fraction in different thermal barrier coating systems after hot corrosion test	41
2.24	YVO ₄ crystals with high number on the YSZ + normal Al ₂ O ₃ coating after hot corrosion test	42
2.25	Formation mode of plasma sprayed coatings structure	43
2.26	Lamellar structure with high interconnected pinholes in plasma sprayed thermal barrier coatings	44
2.27	Cross section of thermal barrier coating, fabricated by EB-PVD method. Columnar structure can be clearly seen in this figure	45
2.28	Cross section of a two-layer FGM coating	47
2.29	Cross section of a five-layer FGM coating	47
2.30	a) air plasma sprayed YSZ coating surface before laser treatment b) air plasma sprayed YSZ coating surface after laser treatment	49
2.31	Comparison of oxygen diffusion coefficient in different oxide ceramics	51
3.1	The flow chart of research methodology	53

3.2	Rotary-evaporator device	57
3.3	Planetary Ball Mill device (PM 400)	58
3.4	The grinding jars of planetary ball mill device (PM 400)	58
3.5	Glove box	59
3.6	Fixture for sustaining the substrates during air plasma spraying process; a) total view b) top view c) front view	60
3.7	The shot blast machine	61
3.8	3MB gun	62
3.9	The air plasma spray (APS) machine	62
3.10	Air plasma spraying (APS) method; a) adjusting plasma flame b) air plasma spraying in length side c) air plasma spraying in width side	62
3.11	The geometry of layers in normal TBC system (Inconel 738/normal NiCrAlY/normal YSZ)	64
3.12	The geometry of layers in nano TBC system (.Inconel 738/Nano NiCrAlY/Normal YSZ)	65
3.13	The geometry of the layers in normal TBC system (Inconel 738/Normal NiCrAlY/Normal YSZ/Normal Al ₂ O ₃)	66
3.14	The geometry of the layers in nano TBC system (Inconel 738/Nano NiCrAlY/Normal YSZ/Nano Al ₂ O ₃) as a novel system	66
3.15	The geometry of the layers in nano TBC system (Inconel 738/Normal NiCrAlY/Nano YSZ)	67
3.16	Formation of an even film of corrosive material on the coating surface keeping 3-4 mm distance from the edge	69
3.17	Schematic diagram of each cycle of hot corrosion test at 1000°C	69
3.18	SEM machine in UTM (Philips, XL.40, Cam Scan MV 2300, Holland) suitable for low magnification investigation	70

3.19	FESEM machine (Supra-350V) in UTM, suitable for high magnification (nano-scale) investigation	71
3.20	FESEM machine (Hitachi-S 4160)	71
3.21	Image analyzer	73
3.22	Normal NiCrAlY layer on the Ni-based super alloy	74
3.23	Nano NiCrAlY layer on the Ni-based super alloy	74
3.24	XRD machine in UTM	74
4.1	The morphology of NiCrAlY powders before and after milling process; a) as-received NiCrAlY powders b) NiCrAlY powders after 36h of milling	77
4.2	The FESEM images of surface of NiCrAlY powders after milling process at different magnifications; a) X 15.0 K b) X 5.0 K c) X 50.0 K d) X 100 K e) X 60.0 K, f) X 110 K.	78
4.3	X-ray diffraction analysis for A) as-received NiCrAlY powders B) milled NiCrAlY powders for 36h	79
4.4	FESEM images of nano Al ₂ O ₃ powders after granulation at different magnifications; a) X 100 b) X 20 K	80
4.5	EDX analysis of granulated nano Al ₂ O ₃ powders	81
4.6	XRD analysis of granulated nano Al ₂ O ₃ powders	82
4.7	SEM images of corrosive salts; a) V ₂ O ₅ b) Na ₂ SO ₄ powders	82
4.8	Elemental analysis of corrosive salts; a) V ₂ O ₅ b) Na ₂ SO ₄ powders	83
4.9	XRD analysis of V ₂ O ₅ powders	83
4.10	XRD analysis of Na ₂ SO ₄ powders	84
4.11	Cross section of normal TBC system after air plasma spraying	85
4.12	Surface morphology of as-sprayed normal YSZ coating at different magnifications; a) 500X b) 2000X c, d) 10000X	85
4.13	Elemental analysis of cross sectional view of ((A) normal NiCrAlY / (B) normal YSZ layers).	86

4.14	XRD analysis of normal YSZ surface after air plasma spraying	87
4.15	Surface morphology of as-sprayed normal NiCrAlY layer at low magnifications; a) 100X b) 500X	87
4.16	Surface morphology of as-sprayed normal NiCrAlY layer at high magnification (10000X)	88
4.17	XRD analysis of outer surface of as-sprayed normal NiCrAlY layer	88
4.18	Cross section of nano TBC system (Inconel 738/nano NiCrAlY/ normal YSZ) after air plasma spraying	89
4.19	Surface morphology of as-sprayed nano NiCrAlY layer at low magnifications; a) 400X b) 1000X	89
4.20	Elemental analysis of cross sectional view of ((A) nano NiCrAlY / (B) normal YSZ layers)	90
4.21	Surface morphology of as-sprayed nano NiCrAlY layer at high magnifications; a) 6000X b) 15000X c) 30000X d) 60000X e) 100000X f) 150000X	91
4.22	XRD analysis of outer surface of as-sprayed nano NiCrAlY layer.	92
4.23	Cross section of normal TBC system (Inconel 738/normal NiCrAlY / normal YSZ / normal Al ₂ O ₃)	93
4.24	Surface morphology of as- sprayed normal Al ₂ O ₃ coating at different magnifications; a) 500X b) 1000X c) 25000X	94
4.25	EDX analysis of different layers of normal TBC system after air plasma spraying ((A) normal NiCrAlY / (B) normal YSZ / (C) normal Al ₂ O ₃)	95
4.26	XRD analysis of outer surface of as-sprayed normal Al ₂ O ₃ layer	96
4.27	Cross section of nano TBC system (Inconel 738/nano NiCrAlY / normal YSZ / nano Al ₂ O ₃) after air plasma spraying	97
4.28	EDX analysis of cross section of nano TBC system ((A) nano NiCrAlY / (B)normal YSZ / (C) nano Al ₂ O ₃)	98

	after air plasma spraying	
4.29	Surface morphology of nanostructured NiCrAlY layer at high magnifications; a) 2000X b) 6000X c) 100000X	99
4.30	Surface morphology of nanostructured Al ₂ O ₃ layer after air plasma spraying at different magnifications; a) 1000X b) 2000X c) 5000X d) 25000X e) 50000X	100
4.31	XRD analysis of outer surface of as-sprayed nano Al ₂ O ₃ layer	101
4.32	Cross section of as-sprayed nano YSZ coating; a) a tri model distribution b) columnar grains c) micro and nano equiaxed grains d) semi melted nano powders	102
4.33	Surface morphology of as-sprayed nano YSZ coating at different magnifications; a) 500X b) 1000X c)10000X d) 15000X	103
4.34	Cross section of the as-sprayed TBCs; (a) NiCrAlY/nano YSZ coating (b) NiCrAlY/normal YSZ coating (for comparison with nano TBC system)	104
4.35	Elemental analysis of cross sectional view of nano TBC system; a) Nano YSZ coating b) normal NiCrAlY layer	105
4.36	X-ray diffraction analysis of as-received powders and as-sprayed YSZ coatings; a) normal YSZ powders b) nano YSZ powders c) as-sprayed normal YSZ layer d) as-sprayed nano YSZ layer	106
4.37	SEM micrographs of cross section of coatings after oxidation at 1000°C for 120h; a) normal NiCrAlY/normal YSZ b) nano NiCrAlY/ normal YSZ c) normal NiCrAlY/normal YSZ/normal Al ₂ O ₃ d) nano NiCrAlY/ normal YSZ/nano Al ₂ O ₃ coatings	109
4.38	TGO layer of four types of TBCs after oxidation at 1000°C for 120h at high magnifications; a) normal NiCrAlY/normal YSZ coating b) nano NiCrAlY/normal YSZ coating c) normal NiCrAlY/normal	110

	YSZ/normal Al ₂ O ₃ coating d) nano NiCrAlY/normal YSZ/nano Al ₂ O ₃ coating	
4.39	The EDS analysis of the TGO layer after oxidation at 1000°C for 48h	110
4.40	The FESEM images of TGO layer of normal TBCs after oxidation at 1000°C for 120h; a) there are several protrusions at the interface of TGO/YSZ b) The micro-crack nucleation within the YSZ layer	111
4.41	TGO thickness versus oxidation time at 1000 °C for four types of TBCs	112
4.42	FESEM images from bi-layered TGO in TBC systems with normal TBC after oxidation at 1000°C for 120h; a) normal NiCrAlY /YSZ coating b) normal NiCrAlY/YSZ/normal Al ₂ O ₃ coating c) nano NiCrAlY/YSZ coating	113
4.43	The EDX analysis of bi-layered TGO; the outer layer of TGO (a, b, c, d and e); and the inner layer of TGO (f)	114
4.44	X-ray diffraction analysis of oxide phases on the NiCrAlY layer	115
4.45	Crack formation at the TGO/YSZ interface; a) the spallation of the ceramic layer may occur at the summit of protrusions, b) the progress of horizontal micro-cracks in the ceramic layer during thermal cyclings is due to presence of vertical tensile stresses on the interface of TGO/YSZ layers	117
4.46	FESEM image of TGO layer of nano NiCrAlY/YSZ/nano Al ₂ O ₃ coating after oxidation at 1000°C for 120h	122
4.47	Cross-section of the coatings after hot corrosion test at 1000°C; a, b) conventional YSZ coating c) YSZ as inner layer of YSZ/normal Al ₂ O ₃ coating d) YSZ as inner layer of YSZ/nano Al ₂ O ₃ coating	125
4.48	XRD results for a) normal YSZ coating b) YSZ as	126

	inner layer of YSZ/normal Al ₂ O ₃ coating c) YSZ as inner layer of YSZ/nano Al ₂ O ₃ coating after hot corrosion test at 1000 °C	
4.49	SEM micrographs of YVO ₄ crystals on the surface of coatings; a,b) normal YSZ coating c,d) YSZ as inner layer of (YSZ / normal Al ₂ O ₃) coating e,f) YSZ as inner layer of (YSZ/ nano Al ₂ O ₃) coating after hot corrosion test at 1000°C.	128
4.50	FESEM micrographs of YVO ₄ crystals on the surface of coatings; a) thicker rod/plate crystals in normal YSZ b) thin rod/plate crystals in YSZ as inner layer of (YSZ / normal Al ₂ O ₃) coating c) thinner rod/plate crystals in YSZ as inner layer of (YSZ/ nano Al ₂ O ₃) coating after hot corrosion test	130
4.51	EDX spectrum from the rod shaped crystals of YVO ₄ on the surface of YSZ layer of TBCs	131
4.52	Schematic illustration of corrosive molten salts infiltration into the YSZ layer of different thermal barrier coating systems during hot corrosion process at elevated temperatures	134
4.53	The outward growth of YVO ₄ crystals in conventional YSZ coating which caused additional stresses at the interface of bond coat/YSZ	136
4.54	The TGO layer of TBCs after oxidation at 1000°C for 24 and 48h; a) normal NiCrAlY/YSZ coating b) nano NiCrAlY/YSZ coating after 24h c) normal NiCrAlY/YSZ coating d) nano NiCrAlY/YSZ coating after 48h of oxidation	139
4.55	The EDX analysis of pure TGO layer after pre-oxidation at 1000°C	139
4.56	The TGO thickness versus pre-oxidation time	141
4.57	Cross section of TBCs after 100 cycles at 1150°C; a) nano NiCrAlY/YSZ coating b) normal NiCrAlY/YSZ coating	143

4.58	Bi-layered TGO in TBCs after 200 cycles at 1150°C; a) normal NiCrAlY/normal YSZ coating b) nano NiCrAlY/normal YSZ coating	144
4.59	EDS line-scan analysis of bi-layered TGO in TBC systems after 200 cycles; a) NiO b) CS c) (Cr, Al) ₂ O ₃ d) Al ₂ O ₃	144
4.60	The X-ray diffraction analyses of oxide phases on the surface of bond coat after 200 cycles at 1150°C; a) normal NiCrAlY layer b) nano NiCrAlY layer	146
4.61	The schematic illustration of formation of detrimental mixed oxides (CSN) on the Al ₂ O ₃ (as pure TGO) layer during thermal exposure in air; a) TGO formation including protrusions b) TGO thickening c) micro-cracks formation at the TGO/YSZ interface d) CSNs formation at the Al ₂ O ₃ /YSZ interface e) CSNs growth and micro-cracks propagation in the YSZ layer.	147
4.62	The thickness of bi-layered TGO versus oxidation time for nano NiCrAlY/YSZ and normal NiCrAlY/YSZ coatings after cyclic oxidation at 1150°C	148
4.63	A three stage TGO growth phenomenon during oxidation at elevated temperatures for nano NiCrAlY/YSZ and normal NiCrAlY/YSZ coatings	149
4.64	TGO layer of different thermal barrier coating systems after oxidation at 1000°C for 24h; a) normal NiCrAlY/normal YSZ b) nano NiCrAlY/normal YSZ c) nano NiCrAlY/normal YSZ/nano Al ₂ O ₃ coatings	152
4.65	TGO layer of different thermal barrier coating systems after oxidation at 1000°C for 48h; a) normal NiCrAlY/normal YSZ b) nano NiCrAlY/normal YSZ c) nano NiCrAlY/normal YSZ/nano Al ₂ O ₃ coatings	153
4.66	EDX analysis of the pure TGO layer in the novel coating	153
4.67	TGO thickness versus oxidation time after isothermal pre-oxidation test for three types of thermal barrier	155

	coating systems	
4.68	Cross section of TBCs after 100 of thermal cycles at 1150°C; a) normal NiCrAlY/YSZ b) nano NiCrAlY/YSZ c) nano NiCrAlY/YSZ/nano Al ₂ O ₃ coatings	157
4.69	Bi-layered TGO in three types of TBC systems after 200 of thermal cycles at 1150 °C; a) normal NiCrAlY/YSZ b) nano NiCrAlY/YSZ c) nano NiCrAlY/YSZ/nano Al ₂ O ₃ coatings	160
4.70	EDX analysis of the TGO layer of three types of TBC systems after 200 thermal cycles at 1150° C; a) CSNs b) Al ₂ O ₃ c) NiO d) NiCr ₂ O ₄ (CS) e) Cr ₂ O ₃ f) ZrO ₂	162
4.71	FESEM images of CSNs and Cr ₂ O ₃ after cyclic oxidation test at 1150°C; a) granular NiO b) hexagonal system of NiO c, d) outward growth of NiO e) formation of nano spinels f) cubic NiAl ₂ O ₄ g) Cr ₂ O ₃ h) cubic NiCr ₂ O ₄	163
4.72	X-ray diffraction analysis of formed oxide phases at the BC/YSZ interface of TBCs after cyclic oxidation at 1150°C	164
4.73	Thickness of bi-layered TGO along the BC/TC interface of three types of TBC systems after 100 and 200 of thermal cycles at 1150 °C	165
4.74	A three stage growth phenomenon of the TGO layer in three types of TBC systems during oxidation (pre-oxidation + cyclic oxidation) at elevated temperatures	166
4.75	Schematic illustration of formation and growth of bi-layered TGO in normal TBC systems after oxidation (pre-oxidation +cyclic oxidation) test	167
4.76	Schematic illustration of formation and growth of bi-layered TGO in nano TBC systems after oxidation (pre-oxidation +cyclic oxidation) test	169
4.77	CSNs at the Al ₂ O ₃ /YSZ interface of nano TBC systems after 200 of thermal cycles at 1150°C; a) nano	170

	NiCrAlY/YSZ coating b) nano NiCrAlY/YSZ/nano Al ₂ O ₃ coating.	
4.78	Surface of YSZ layers after hot corrosion test; a) surface of nano YSZ layer b) surface of normal YSZ layer after spallation	174
4.79	EDX analysis of YVO ₄ crystals in normal and nano YSZ coatings	175
4.80	XRD analysis from surface of YSZ layer after hot corrosion test; a) nano YSZ layer b) normal YSZ layer after spallation	175
4.81	Schematic illustration of hot corrosion process in nano YSZ layer; a) penetrated corrosive fused salts into the entire thickness of the nano YSZ layer b) depletion of stabilizer (Y ₂ O ₃) in zirconia and followed by the phase transformation of tetragonal zirconia to monoclinic zirconia c) easy transformation of zirconia to fully monoclinic and formation of YVO ₄ crystals which have outward growth d, e) SEM images of YVO ₄ crystals at different magnifications	177
4.82	Schematic illustration of hot corrosion process in normal YSZ layer; a) penetrated corrosive fused salts into the entire thickness of the nano YSZ layer b) depletion of stabilizer (Y ₂ O ₃) in zirconia and followed by the phase transformation of tetragonal zirconia to monoclinic zirconia c) easy transformation of zirconia to fully monoclinic and formation of YVO ₄ crystals which have outward growth d, e) FESEM and SEM images of YVO ₄ crystals at different magnifications	178
4.83	Chemical composition of ZrV ₂ O ₇ on the YSZ layer after hot corrosion test at 1000°C	179
4.84	Cross section of coatings after high temperature oxidation at 1000°C for 12h; a) NiCrAlY /nano YSZ coating b) NiCrAlY /normal YSZ coating c) the presence of unique structure of nano YSZ coating over	182

	the TGO layer	
4.85	Cross section of coatings after high temperature oxidation test at 1000°C for 24h; a) NiCrAlY /normal YSZ coating b) NiCrAlY /nano YSZ coating c) CSNs formation on the Al ₂ O ₃ oxide scale in NiCrAlY /normal YSZ coating d) CSNs formation on the Al ₂ O ₃ oxide scale in NiCrAlY /nano YSZ coating	183
4.86	Cross section of coatings after high temperature oxidation at 1000°C for 48h; a) NiCrAlY /normal YSZ coating b) NiCrAlY /nano YSZ coating c) presence of nano grains over the continues TGO layer in NiCrAlY /nano YSZ coating	184
4.87	Cross section of coatings after high temperature oxidation at 1000°C for 120h; a) NiCrAlY /normal YSZ coating b) NiCrAlY /nano YSZ coating c) more CSNs formation on the Al ₂ O ₃ oxide scale in NiCrAlY /normal YSZ coating d) lower CSNs formation on the Al ₂ O ₃ oxide scale in NiCrAlY /nano YSZ coating	185
4.88	EDX analysis of TGO (Al ₂ O ₃) layer in NiCrAlY/nanoYSZ coating after high temperature oxidation test at 1000°C	185
4.89	Micro-cracks formation and growth in the CSNs and protrusions; a) FESEM image of a protrusion at the TGO/YSZ interface of normal TBC system after 120h of high temperature oxidation test at 1000°C b) schematic illustration of progress of horizontal micro-cracks within the ceramic layer and coalescence of formed micro-cracks inside the CSNs (particularly on the protrusions) with discontinuities and pre-existing open micro-cracks in the YSZ layer	187
4.90	TGO thickness versus oxidation time for normal and nano TBC systems after high temperature oxidation test at 1000°C for 120h	188
4.91	EDX analysis of a) inner layer of TGO and, b-f) outer	190

	layer (CSNs) of TGO after high temperature oxidation test at 1000°C for 120h	
4.92	X-ray map from inner and outer layers of TGO after 120h of oxidation at 1000°C	191
4.93	Type of formed oxide phases on the Al ₂ O ₃ oxide scale after 120h of oxidation	192
4.94	Cross section of coatings after per-oxidation at 1000°C for 12h; a) NiCrAlY /normal YSZ coating b) NiCrAlY /nano YSZ coating	195
4.95	Cross section of coatings after pre-oxidation at 1000°C for 24h; a) NiCrAlY /normal YSZ coating b) NiCrAlY /nano YSZ coating	195
4.96	Cross section of coatings after pre-oxidation at 1000°C for 48h; a) NiCrAlY /normal YSZ coating b) NiCrAlY /nano YSZ coating c) pure TGO layer in nano TBC system (NiCrAlY/nano YSZ)	196
4.97	Schematic illustration of oxygen penetration into the nano TBC system and TGO formation during oxidation; a) lower oxygen penetration in nano YSZ layer b) Formation of nearly continuous but thinner Al ₂ O ₃ layer in NiCrAlY/nano YSZ coating during isothermal pre-oxidation	198
4.98	Schematic illustration of oxygen penetration into the normal TBC system and TGO formation during oxidation; a) more oxygen diffusion in normal YSZ layer b) Formation of discontinuous but thicker Al ₂ O ₃ layer in NiCrAlY/normal YSZ coating during isothermal pre-oxidation	199
4.99	X-ray map of oxidized regions (containing mixed oxides (1) which are surrounded by Al ₂ O ₃ layer (2)) after isothermal pre-oxidation at 1000°C	200
4.100	TGO thickness versus pre-oxidation time for NiCrAlY/normal YSZ and NiCrAlY/nano YSZ coatings	201

4.101	Cross section of coatings after 30 thermal cycles at 1150°C; a, c) NiCrAlY /normal YSZ coating b, d) NiCrAlY /nano YSZ coating	203
4.102	Cross section of coatings after 50 thermal cycles at 1150°C; a, c, e) NiCrAlY /nanoYSZ coatings b, d, f) NiCrAlY /normal YSZ coatings	204
4.103	Cross section of coatings after 100 thermal cycles at 1150°C; a, c) NiCrAlY /normal YSZ coatings b, d) NiCrAlY /nano YSZ coatings e) X-ray map of NiCrAlY /nano YSZ coating (d)	205
4.104	Cross section of coatings after 200 thermal cycles at 1150°C; a) NiCrAlY /nano YSZ coating, in addition to its X-ray map b) NiCrAlY /normal YSZ coating, in addition to its X-ray map	206
4.105	Horizontal micro-cracks growth within the CSNs; the coalescence of micro- cracks and formation of a large crack in the YSZ layer near the interface in a cleavage mode.	207
4.106	Cross section of NiCrAlY/nano YSZ coating after 50 thermal cycles at 1150°C; (1) nearly continues and thinner TGO layer, and (2) the presence of unique structure of nano YSZ coating (particularly nano zones) top of the TGO layer	209
4.107	X-ray map of bi-layered TGO (containing inner (A) and outer (B) layers) in NiCrAlY/nano YSZ coating after 200 thermal cycles at 1150°C	210
4.108	X-ray map and EDX analysis of inner and outer layers of the TGO in NiCrAlY/normal YSZ coating after 200 thermal cycles at 1150°C	211
4.109	XRD analysis of formed oxide phases on the bond coat (NiCrAlY layer) after 200 thermal cycles at 1150°C	212
4.110	TGO thickness versus oxidation (pre-oxidation + cyclic oxidation) time for NiCrAlY/normal YSZ and NiCrAlY/nano YSZ coatings	212

- 4.111 TGO texture during oxidation; a, b) Al_2O_3 oxide scale (as pure TGO) with columnar grains (columnar zone or CZ), in addition to somewhat equiaxed grains (equiaxed zone or EZ) a, e) particles of YAG ((Y–Al–O) precipitates) along columnar grain boundaries of Al_2O_3 and its EDX analysis c, d) equiaxed grains of CSNs with cubic crystalline structure d) NiO with hexagonal structure 214

LIST OF ABBREVIATIONS

APS	- Air Plasma Spray
BC	- Bond Coat
CZ	- Columnar Zone
CVD	- Chemical Vapor Deposition
CTE	- Coefficient of Thermal Expansion
EDX	- Energy Dispersive Spectroscopy
EZ	- Equiaxed Zone
EB-PVD	- Electron Beam- Physical Vapor Deposition
EBSD	- Electron Backscatter Diffraction Analysis
FESEM	- Field Emission Scanning Electron Microscope
PSZ	- Partially Stabilized Zirconia
SEM	- Scanning Electron Microscope
TEM	- Transmission Electron Microscope
TGO	- Thermally Grown Oxide
TBC	- Thermal Barrier Coating
TC	- Top Coat
XRD	- X-ray Diffraction
YSZ	- Yttria Stabilized Zirconia
TBCs	- Thermal Barrier Coating System
FGM	- Functionally Graded Materials
LPHS	- Laser Plasma Hybrid Spraying

LIST OF APPENDICES

APPENDIX	TITLE	PAGE
A	List of Papers	231
B	Used Materials in This Project	233

CHAPTER 1

INTRODUCTION

1.1 Research Background

Gas turbines have been claimed to be one of the most important systems for generating energy at the present and the future. Most research activities on gas turbines have been carried out, in order to enhance the thermal efficiency and durability of gas turbines components. The efficiency and durability of turbine blades can be increased by using high strength materials and protective coatings at high temperature applications [1, 2].

Ni or Co based superalloys were developed during 1950-1970. The Ni-based superalloys are usually used in fabrication of turbine blades and hot sections of gas turbines. Depending on the type of turbine, the temperature of external gases from the combustor can range between 800-1200°C. Under these conditions, superalloy would be reacted by high temperature oxidation and corrosion at elevated temperatures [3].

Additionally, Ni- based superalloys do not have adequate resistance at above ambient condition [4]. So, surface protection of gas turbine blades is very important using highly resistant ceramic coatings. The following coatings could improve high temperature oxidation and corrosion resistances of gas turbine blades at elevated temperatures:

(1) Diffusion coatings: the aluminum can diffuse into the substrate surface. These coatings are usually applied on substrate using Diffusion – Slurry, Powdery Sementasion and CVD methods.

(2) Overlay coatings: the principal chemical composition of these coatings is: MCrAlY (M=Ni, Co or both of them) which is usually applied on the blades via plasma spray or EB-PVD methods.

(3) Thermal barrier coating (TBC): these coatings have low thermal conductivity. They could significantly reduce the overall substrate (Ni- based superalloy) temperature [4-6].

TBCs could significantly increase the efficiency and durability of hot sections of gas turbines because zirconia has lower thermal conductivity in comparison with other ceramics [4]. If this coating is applied on the substrate, then the temperature of internal gases inside the combustor of gas turbines will be increased. It means that, the substrate temperature would not be altered [5].

The first TBC was applied on the engine components of aircraft in 1960. This coating had several problems such as ZrO_2 instability and poor bonding between the substrate and the ceramic thermal barrier coating [2]. These problems were then solved during 1970 – 1980 using (a) YSZ as a thermal barrier layer due to its low thermal conductivity, and (b) metallic bond coat MCrAlY (M = Ni, Co or mixture of these two) which was employed to improve the adhesion between the ceramic top-coat and the substrate. MCrAlY layer is an oxidation-resistant material.

Additionally, MCrAlY plays a major role in providing a rough and adherent surface for applying thermal barrier coatings and provides protection for the alloy (substrate) from further oxidation [7]. Other researches were carried out by some investigators during 1980-2007, which are: (a) FGM (Functionally Graded Materials) coatings: this coating increased the mechanical properties of coating [8, 9], (b) CeO_2 stabilizer that can be added to the ceramic thermal barrier layer, in order to improve

thermal shock resistance, and (c) remelting the ceramic layer using laser which reduced the oxygen infiltration into the TBCs [10].

Additionally, other researchers also investigated other aspects of TBCs during 2002-2011 which are: (a) to replace zirconia (ZrO_2) with other ceramic materials in order to obtain lowest thermal conductivity and highest stability [11, 12], (b) to reduce oxygen diffusion and fused salts infiltration into the YSZ layer using normal Al_2O_3 as a third layer over the YSZ coating [11-19], and (c) to reduce the TGO growth and internal oxidation of the bond coat using nano crystalline NiCrAlY layer as bond coat in a TBC system [20-23]. In this research, it is expected that oxidation and hot corrosion resistances of TBCs at elevated temperatures will be considerably increased. This involves the use of nanostructured NiCrAlY layer as bond coat (via formation of continuous Al_2O_3 layer) in a TBC system with nanostructured Al_2O_3 as a third layer (as an infiltration barrier on the YSZ coating).

1.2 Problem Statement

Listed are the current major problems associated with conventional TBCs:

(a) TGO formation and growth in TBCs: an oxidized scale can be formed on the bond coat (BC) which is termed thermally grown oxide layer which is mainly related to the oxygen diffusion through the top coat towards the bond coat at elevated temperatures by micro-cracks and interconnected pinholes inside the top coat (TC) (via gas infiltration mechanism) [24]. It was found that the growth of the TGO layer plays an important role in the failure of TC during thermal exposure in air [25], (Figure 1.1).

The increase in TGO thickness during the oxidation process is accompanied by the evolution of stress at the BC / YSZ interface. This stress would cause the delamination of the coating at the interface of the BC / YSZ. It was found that the stresses in TBC will increase with a growing TGO layer [26].

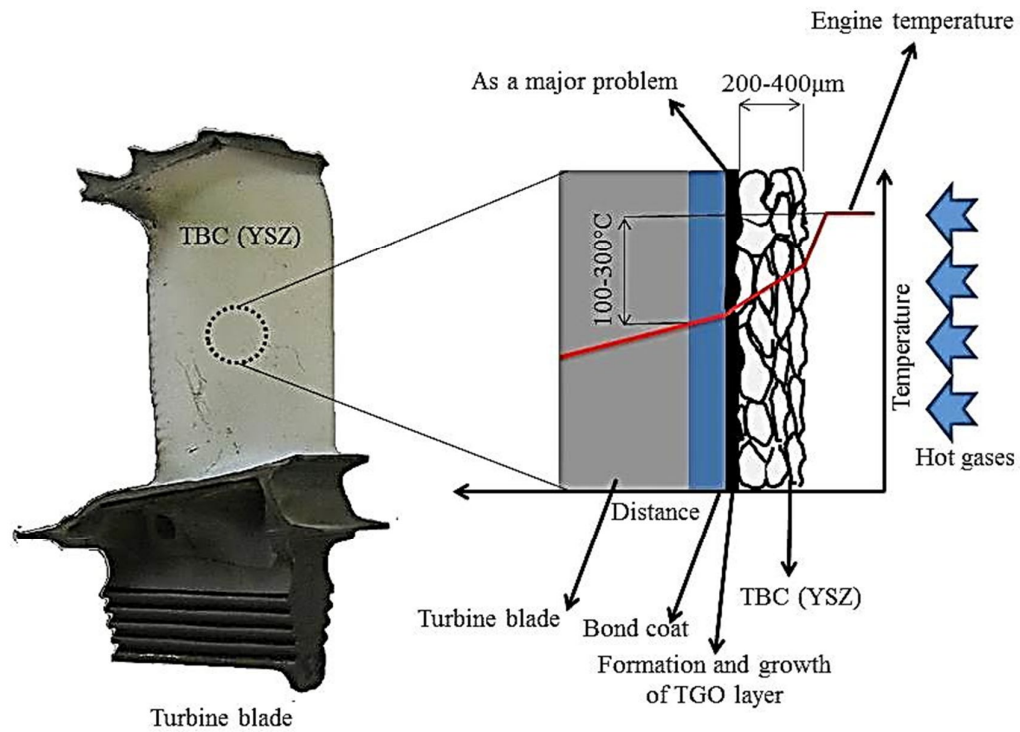


Figure 1.1: Schematic illustration of a normal thermal barrier coating system in addition to thermally grown oxide (TGO) layer. The temperature gradient during engine operation can be also observed.

(b) CSNs formation and growth on the Al_2O_3 oxide scale (as pure TGO): The mixed oxides formation on the Al_2O_3 oxide scale (as pure TGO) has been reported by the other investigators [25-27]. These complex oxides (CSNs) contain chromia $(\text{Cr,Al})_2\text{O}_3$, spinel $\text{Ni}(\text{Cr,Al})_2\text{O}_4$ (CS) and nickel oxide NiO [28-31] which may be formed via a solid state reaction along with this TGO (Al_2O_3) layer in plasma sprayed TBC systems [32, 33].

CSNs are also believed to be detrimental to TBC durability during service at higher temperatures [26]. In this regard, it was reported that the maximum radial stress of bi-layered TGO (Al_2O_3 /detrimental mixed oxides) is about five times and the difference of maximum axial stress is about 10 times larger than mono-layered TGO (Al_2O_3) [26]. The formation of harmful oxides would provoke micro-cracks

nucleation during thermal exposure in air, leading to premature TBC failure during extended thermal exposure in air [26, 29-31].

The majority of previous researches described the failure mechanisms of TBCs due to TGO growth especially internal oxidation of BC during high temperature oxidation [30, 34]. Therefore, the main purpose of this research is to obtain a new coating to reduce the growth of the TGO layer during pre-oxidation (as a thinner and continuous Al_2O_3 layer) and to suppress the formation and growth of detrimental mixed oxides on the Al_2O_3 (as pure TGO) layer during thermal shocks.

(c) TC (TBC) deterioration during hot corrosion process: Low quality fuels usually contain impurities such as Na and V which lead to the formation of Na_2SO_4 and V_2O_5 corrosive salts on the coating of turbine blades [14]. These corrosive fused salts can penetrate into the entire thickness of YSZ through splat boundaries and other YSZ coating defects such as micro-cracks and open pores during hot corrosion process [34]. The penetrated salts can then react with yttria (the stabilizer component of YSZ). So, the depletion of the stabilizer and phase transformation of tetragonal zirconia to monoclinic zirconia and followed by YVO_4 crystals formation can occur in a very rapid and effective manner during cooling [14, 34]. This phase transformation is accompanied by 3–5% rapid volume expansion, leading to cracking and spallation of TBC [35]. So, the reduction of hot corrosion products (by using nanostructured Al_2O_3 coating) in the YSZ layer can be expected as a major factor for increasing the lifetime of TBCs during hot corrosion process.

1.3 Purpose of the Study

In this research, it is anticipated that the aforementioned problems to be considerably decreased using a TBC system consisting of nanostructured NiCrAlY (manufactured using planetary ball mill) as bond coat (BC) and YSZ/ nano Al_2O_3 (using granulated nano Al_2O_3 powders) coating as top coat (TC). In this regard, the nanostructured NiCrAlY layer would create a continuous and dense layer of Al_2O_3 on the BC which is a strong barrier for the oxygen penetration into the NiCrAlY

layer [20]. Nanostructured Al_2O_3 top coat over the YSZ layer will significantly lessen the oxygen diffusion and corrosive molten salts infiltration into the YSZ layer at higher temperatures. This phenomenon may be originated from the compactness of the nanostructure that was observed in the nanostructured YSZ coating which was mainly composed of nano zones and fully molten parts [36].

It is worth mentioning that the Al_2O_3 crystal lattice on the YSZ layer would resist the oxygen diffusion into the YSZ layer [13, 15]. Previous studies also showed that the dense alumina layer over the YSZ coating can lessen the oxygen partial pressure at the BC/YSZ interface and can prevent further formation of deleterious oxides within the BC [16, 18].

In later studies [32, 37], it was found that a continuous Al_2O_3 layer could develop at the ceramic/bond coat interface in air plasma-sprayed normal TBC systems under a low oxygen pressure conditions (furnace with low oxygen pressure). This continues and thin Al_2O_3 (TGO) layer could diminish the growth of CSNs in the normal TBC system during subsequent thermal exposure in service [37]. In this research, a new TBC system is required to create a dense, continuous and thinner Al_2O_3 layer on the BC during pre-oxidation in air, in order to diminish the formation and growth of Ni (Cr,Al) $_2\text{O}_4$ (spinel) and NiO oxides on the alumina oxide scale during thermal cycles in air. In other words, it is expected that nano TBC systems after a pre-oxidation could considerably improve oxidation behavior of normal TBC systems at elevated temperatures.

It was observed that the protective Al_2O_3 layer on the YSZ coating can remarkably reduce the molten salts infiltration into the YSZ layer and can substantially lessen the depletion of stabilizer (Yttria) from this layer during the hot corrosion process. So, the percentage of monoclinic ZrO_2 and YVO_4 crystals (as hot corrosion products) was reduced in YSZ/ normal Al_2O_3 coating compared to that of conventional YSZ coating [14, 38]. In this research, it is expected that the usage of nanostructured Al_2O_3 layer over the YSZ coating could significantly reduce the corrosive molten salts penetration within the YSZ layer and could lessen hot

corrosion products in the YSZ as inner layer of YSZ/nano Al_2O_3 coating during the hot corrosion process.

Recently, NiCrAlY/nano YSZ coating showed better high temperature oxidation (according to the TGO thickness) and corrosion (according to hot corrosion products values) resistance compared to NiCrAlY/normal YSZ coating [36, 39]. This is because of the presence of nanostructured YSZ layer (with lower pinholes and micro-cracks) in the nano TBC system. But, the formation and growth of CSNs (NiO , $\text{Ni}(\text{Cr,Al})_2\text{O}_4$, $(\text{Cr, Al})_2\text{O}_3$) have not been studied yet in the NiCrAlY/nano YSZ coating during extended thermal exposure in air. Therefore, it can be speculated that the CSNs formation and growth in NiCrAlY/nano YSZ coating to be considerably suppressed in comparison with NiCrAlY/normal YSZ coating during cyclic oxidation (thermal shocks).

1.4 Objectives of the Study

The main objectives in the present research are as follows:

1) To lessen the oxygen diffusion (getting TGO (Al_2O_3) layer with lowest thickness) and also molten corrosive salts infiltration (according to hot corrosion products values) into the YSZ layer by using nanostructured Al_2O_3 top coat over the YSZ layer during high temperature oxidation and corrosion.

2) To further reduce oxidation effect (bi-layered TGO thickness) using nanostructured NiCrAlY as bond coat (BC) and YSZ/ nano Al_2O_3 coating as top coat (TC) in a TBC system, simultaneously during cyclic oxidation (thermal shocks).

1.5 Scopes of Work

- In order to prepare the nanostructured NiCrAlY powders, commercial Ni22Cr10Al1Y powders would be milled using planetary ball mill device for 36h [20, 21, 40 and 41].

- The nanostructured NiCrAlY powders (as bond coat) will be then applied on the base metal by APS method.

- In order to produce nano NiCrAlY/normal YSZ/nano Al₂O₃ coating (Figure 1.2), normal YSZ layer will be sprayed on the nanostructured NiCrAlY layer and followed by granulated nano Al₂O₃ powders will be then deposited on the YSZ layer.

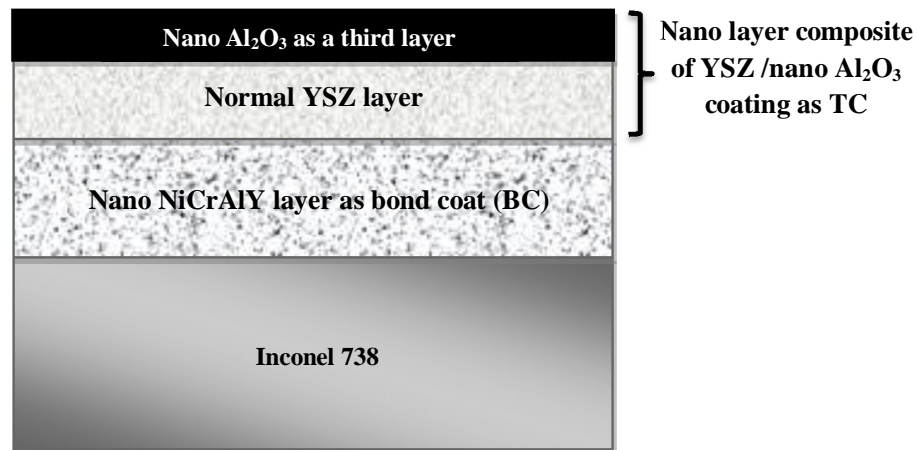


Figure 1.2: Schematic illustration of cross section of air plasma sprayed nano NiCrAlY/normal YSZ/nano Al₂O₃ coating on the Ni-based superalloy (as a novel TBC system) in this research.

So, it is anticipated that the new coating (See Figure 1.2) to form a thinner and fully continuous Al₂O₃ layer at the BC/YSZ interface during pre-oxidation and to diminish the formation and growth of detrimental mixed oxides on the Al₂O₃ (as pure TGO) layer during cyclic oxidation (thermal shocks). In this research, it is also expected that the nanostructured Al₂O₃ layer over the YSZ coating could significantly reduce the corrosive molten salts penetration within the YSZ layer and could lessen hot corrosion products in the YSZ as inner layer of YSZ/nano Al₂O₃ coating during hot corrosion process. On the other hand, the reduction of hot corrosion products (YVO₄ crystals and monoclinic zirconia) in the YSZ layer is a major factor for increasing the lifetime of TBCs during hot corrosion process which was observed in the triple layered TBCs [38].

- Normal NiCrAlY layer (as bond coat), normal and nano YSZ layers (as top coats) will be eventually applied on the base metal (Inconel 738) using APS method. On the whole, five types of TBCs will be produced which consist of: (1) Inconel 738/normal NiCrAlY/normal YSZ (normal TBCs), (2) Inconel 738/normal NiCrAlY/normal YSZ/normal Al_2O_3 (normal TBCs), (3) Inconel 738/nano NiCrAlY/normal YSZ (nano TBCs), (4) Inconel 738/nano NiCrAlY/normal YSZ/nano Al_2O_3 (as a novel nano TBCs), and (5) Inconel 738/normal NiCrAlY/nano YSZ (nano TBCs).

- The air plasma sprayed normal and nano TBC systems will be evaluated by pre-oxidation (at 1000°C for 48h), high temperature oxidation (at 1000°C for 120h), cyclic oxidation (or thermal shocks at 1150°C) and hot corrosion (at 1000°C) tests.

- Microstructural characterization of the coatings before and after tests will be performed using SEM, EDS, FESEM, XRD, and X-ray mapping.

1.6 Organization of Thesis

This thesis consists of five chapters. Chapter 1 provides an introduction to the study. The background of the study, problem statement, objectives and scopes of the study and organization of thesis are presented in this chapter. In the Chapter 2, normal thermal barrier coating system and its problems in the service would be comprehensively introduced. In the meantime, recent research activities about improvement of TBCs at elevated temperatures are reviewed. Chapter 3 is concerned with the research methodology for this study. In this chapter, the experimental steps from providing feed Stokes until microstructural characterization of samples are discussed in detail. There are 7 sub chapters in the Chapter 4. In this chapter, 1) microstructural characterization of the feed Stokes and as-sprayed coatings, 2) improvement of thermally grown oxide layer in thermal barrier coating systems with nano alumina as a third layer during isothermal oxidation, 3) investigation of hot corrosion resistance of YSZ/ nano Al_2O_3 coating at 1000 °C, 4) role of formation of continues thermally grown oxide layer on the nanostructured NiCrAlY bond coat during thermal exposure (pre-oxidation + cyclic oxidation) in air, 5) formation of a

thinner and continues Al_2O_3 layer in nano thermal barrier coating systems for the suppression of Spinel growth on the Al_2O_3 oxide scale during cyclic oxidation, 6) high temperature oxidation and corrosion behavior of thermal barrier coating systems with nanostructured YSZ as top coat, and 7) formation and effect of nearly continuous but thinner thermally grown oxide scale in NiCrAlY/nanostructured YSZ coating during oxidation (pre-oxidation + cyclic oxidation) test would be comprehensively discussed. Chapter 5 summarizes all the results and discussion in this research and some recommendations for the future work are also made.

REFERENCES

1. Schmitt. T. K. G, Hertter. M (1999). Improved oxidation resistance of thermal barrier coatings. *Surface and Coatings Technology*. 120–121, 84–88.
2. Brandl. W, Grabke. H. J, Toma. D, Kruger. J (1996). The oxidation behavior of sprayed MCrAlY coatings. *Surface and Coatings Technology*. 86-87 (part 1), 41-47.
3. Schulz. U, Leyens. C, Fritscher. K, Peters. M, Saruhan-Brings. B, Lavigne. O, Dorvaux. Jean-M, Poulain. M, Mévrel. R, Caliez. M (2003). Some recent trends in research and technology of advanced thermal barrier coatings. *Aerospace Science and Technology*. 7 (1), 73–80.
4. Jeanine. T (1994). Protective coatings in the gas turbine engine. *Surface and Coatings technology*. 68-69, 1-9.
5. Haynes. J. A, Ferber. M. K, Porter. W. D (2000). Thermal Cycling Behavior of Plasma-Sprayed Thermal Barrier Coatings with Various MCrAlX Bond Coats. *Thermal Spray Technology*. 9 (1), 38-48.
6. Sohn. Y. H, Kim. J. H (2001). Thermal cycling of EB-PVD/MCrAlY thermal barrier coatings: I. Microstructural development and spallation mechanisms. *Surface and Coatings Technology*. 146 –147, 70–78.
7. Seung. Y, Lee. I. G, Lee. D. Y, Kim. D. J., Kim. S, Lee. K (2002). High-temperature properties of plasma-sprayed coatings of YSZ/NiCrAlY on Inconel substrate. *Materials Science and Engineering A*. 332 (1-2), 129–133.
8. Kawasaki. A, Watanabe. R (2002). Thermal fracture behavior of metal/ceramic functionally graded materials. *Engineering Fracture Mechanics*. 69 (14-16), 1713–1728.
9. Shanmugavelayutham. G, Kobayashi. A (2007). Mechanical properties and oxidation behavior of plasma sprayed functionally graded zirconia–alumina thermal barrier coatings. *Materials Chemistry and Physics*. 103 (2-3), 283–289.

10. Batista. C, Portinha. A, Ribeiro. R. M, Teixeira. V, Oliveira. C. R (2006). Evaluation of laser-glazed plasma-sprayed thermal barrier coatings under high temperature exposure to molten salts. *Surface and Coatings Technology*. 200 (24) 6783–6791.
11. Park. S.Y, Kim. J. H, Kim. M. C, Song. H. S, Park. C. G (2005). Microscopic observation of degradation behavior in Yttria and Ceria stabilized zirconia thermal barrier coatings under hot corrosion. *Surface and Coatings Technology*. 190 (2-3), 357– 365.
12. Ma. B, Yao. L (2009). Characterization of ceria–yttria stabilized zirconia plasma-sprayed coatings. *Applied Surface Science*. 255 (16), 7234–7237.
13. Saremi. M, Afrasiabi. A(2008). Microstructural analysis of YSZ and YSZ/Al₂O₃ plasma sprayed thermal barrier coatings after high temperature oxidation. *Surface and Coatings Technology*. 202 (14), 3233–3238.
14. Chen. Z, Wu. N. Q, Singh. J, Mao. S. X (2003). Effect of Al₂O₃ overlay on hot-corrosion behavior of Yttria-Stabilized Zirconia coating in molten sulfate-vanadate salt. *Thin Solid Films*. 443 (1-2), 46–52.
15. Widjaja. S, Limarga. A. M, Yip. T. H (2002). Oxidation behavior of a plasma-sprayed functionally graded ZrO₂/Al₂O₃ thermal barrier coating. *Materials Letters*. 57 (3), 628–634.
16. Limarga. A. M, Widjaja. S, Yip. T. H, The. L K (2002). Modeling of the effect of Al₂O₃ interlayer on residual stress due to oxide scale in thermal barrier coatings. *Surface and Coatings Technology*. 153 (1) 16–24.
17. Zhao. X, Hashimoto. T, Xiao. P (2006). Effect of the top coat on the phase transformation of thermally grown oxide in thermal barrier coatings. *Scripta Materialia*. 55 (11), 1051–1054.
18. Gao. J, He. Y, Wang. D (2011). Preparation of YSZ/Al₂O₃ micro-laminated coatings and their influence on the oxidation and spallation resistance of MCrAlY alloys. *European Ceramic Society*. 31 (1-2) 79-84.
19. Limarga. A. M, Widjaja. T. S, Yip. T. H (2005). Mechanical properties and oxidation resistance of plasma-sprayed multilayered Al₂O₃/ZrO₂ thermal barrier coatings. *Surface and Coatings Technology*. 197 (1), 93– 102.
20. Zhang. Q, Li. C. J, Xin. C. L, Yang. G. J, Lui. S. C (2008). Study of oxidation behavior of nanostructured NiCrAlY bond coatings deposited by cold spraying. *Surface and Coatings Technology*. 202 (14), 3378–3384.

21. Ajdelsztajn. L, Tang. F, Kim. G. E, Provenzano. V, Schoenung. M (2005). Synthesis and Oxidation Behavior of Nanocrystalline MCrAlY Bond Coatings. *Thermal Spray Technology*. 14 (1) 23-30.
22. Kim. G. E, Addona. T, Richer. P, Jodoin. B, Al-Mathami. A (2010). Characterization and Evaluation of Nanostructured Bond Coats from Non-cryogenically Milled Feedstock. *Thermal Spray Technology*. 112 (2) 29–33.
23. Ajdelsztajn. L, Hulbert. D, Mukherjee. A, Schoenung. J. M (2007). Creep deformation mechanism of cryomilled NiCrAlY bond coat material. *Surface and Coatings Technology*. 201 (24) 9462-9467.
24. Fox. A. C, Clyne. T. W (2004). Oxygen transport by gas permeation through the zirconia layer in plasma sprayed thermal barrier coatings. *Surface and Coatings Technology*. 184 (2-3), 311–321.
25. Chen. W.R, Wu. X, Marple. B.R, Patnaik. P.C (2005). Oxidation and crack nucleation/growth in an air-plasma-sprayed thermal barrier coating with NiCrAlY bond coat. *Surface and Coatings Technology*. 197 (1), 109– 115.
26. Ni. L.Y, Liu. C, Huang. H, Zhou. C. G (2011). Thermal Cycling Behavior of TBCs with HVOF NiCrAlY. *Thermal Spray Technology*. 20 (5), 1133–1138.
27. Prescott. R, Graham. M. J (1992). The formation of Aluminum oxide scales on high-temperature alloys. *Oxidation of Metals*. 38 (3-4), 233-254.
28. Rabiei. A, Evans. A. G (2000). Failure Mechanisms Associated with the thermally grown oxide in plasma-sprayed thermal barrier coatings. *Acta materialia*. 48 (15), 3963–3976.
29. Mumm. D. R, Evans. A. G (2000). On the role of imperfections in the failure of a thermal barrier coating made by Electron Beam Deposition. *Acta materialia*. 48 (8), 1815-1827.
30. Chen. W. R, Wu. X, Marple. B. R, Patnaik. P. C (2006). The growth and influence of thermally grown oxide in a thermal barrier coating. *Surface and Coatings Technology*. 201(3-4), 1074–1079.
31. Lee. C. H., Kim. H. K., Choi. H. S, Ahn. H. S (2000). Phase transformation and bond coat oxidation behavior of plasma-sprayed zirconia thermal barrier coating. *Surface and Coatings Technology*. 124(1), 1–12.
32. Chen. W. R, Wu. X, Dudzinski. D, Patnaik. P. C (2006), Modification of oxide layer in plasma-sprayed thermal barrier coatings. *Surface and Coatings Technology*. 200 (20-21), 5863–5868.

33. Liang. G.Y, Zhu. C, Wu. X.Y, Wu. Y (2011). The formation model of Ni-Cr oxides on NiCoCrAlY- sprayed coating. *Applied Surface Science*. 257 (15), 6468-6473.
34. Saremi. M, Afrasiabi. A, Kobayashi. A (2007). Bond coat oxidation and hot corrosion behavior of plasma sprayed YSZ coating on Ni superalloy. *Transaction of JWRI*. 36 (1), 41-45.
35. Chen. H. C., Liu. Z. Y., Chuang. Y. C (1993). Degradation of plasma-sprayed alumina and zirconia coatings on stainless steel during thermal cycling and hot corrosion. *Thin solid Films*. 223(1), 56–64.
36. Saremi. M, Keyvani. A, Sohi. M. H (2012). Hot corrosion resistance and mechanical behavior of atmospheric plasma sprayed conventional and nanostructured zirconia coatings. *International Journal of Modern Physics*. 5, 720–727.
37. Chen. W. R, Wu. X, Marple. B. R, Lima. R. S, Patnaik. P. C (2008). Pre-oxidation and TGO growth behavior of an air-plasma-sprayed thermal barrier coating. *Surface and Coatings Technology*. 202 (16), 3787–3796.
38. Afrasiabi. A, Saremi. M (2008). A comparative study on hot corrosion resistance of three types of thermal barrier coatings: YSZ, YSZ+Al₂O₃ and YSZ/Al₂O₃. *Materials Science and Engineering A*. 478 (1-2), 264–269.
39. Girolamo. G. Di, Marra. F, Blasi. C, Serra. E (2011). Microstructure, mechanical properties and thermal shock resistance of plasma sprayed nanostructured zirconia coatings. *Ceramics International*. 37 (7), 2711-2717.
40. Hussain. M. S, Ababtian. M .A (2009). Nano-composites NiCrAl (MCrAl) ternary alloy powder synthesized by mechanical alloying. *Journal of Nano Research*. 6, 169-176.
41. Hussain. M. S., Swailem. S. A, A. Hala (2009). Advanced nano composites for high temperature aero-engine/turbine components. *Journal of Nano Manufacturing*. 4 (1-4), 248-256.
42. Kewther. A, Yilbas. B. S, Hashmi. M. S. J (2001). Corrosion Properties of Inconel 617 Alloy after Heat Treatment at Elevated Temperature. *Materials Engineering and Performance*. 10 (1), 108-113.
43. Nesb. J. A (1990). Thermal response of various thermal barrier coatings in high heat flux rocket engine. *Surface and Coatings Technology*. 43/44 (part 1), 458-469.

44. Bengtsson. P, Persson. C (1997). Modeled and measured residual stresses in plasma sprayed thermal barrier coatings. *Surface and coating technology*. 92 (1-2) 78-86.
45. Nicoll. A. R. Wahl. G (1991). The effect of alloying additions on M-Cr-Al-Y systems-An experimental study. *Thin Solid Films*. 95 (1), 21-34.
46. Kvernes. I, Lugscheider. E, Lindblorn. Y (1992). Protection materials: coatings for thermal barrier and wear resistance. *Proceedings of the 2nd European symposium engineering ceramics*. England, 280-285.
47. Smeggil. J. L (1987). Some comments on the role of yttrium in protective oxide scale adherence. *Materials Science Engineering*. 87, 261-265.
48. Ge. Q. L, Lei. T. C, Mao. J. F, Zhou. Y (1993). In situ transmission electron microscopy observations of the tetragonal-to-monoclinic phase transformation of zirconia in $\text{Al}_2\text{O}_3\text{-ZrO}_2$ (2 mol % Y_2O_3) composite. *Journal of Materials Science Letters*. 12, 819-822.
49. Joshi. S. V, Sivatava. M. P (2000). On the thermal cyclic life of plasma sprayed Yttria-Stabilized Zirconia coatings. *Surface and Coating Technology*. 56, 215-224.
50. Seo. D, Ogawa. K, Suzuki. Y, Ichimura. K, Shoji. T, Murata. S (2008). Comparative study on oxidation behavior of selected MCrAlY coatings by elemental concentration profile analysis. *Applied Surface Science*. 255 (5, part 2), 2581–2590.
51. Straussa, D, Müller. U. G, Schumacher. G, Engelkob. V, Stammc. W, Clemensd. D, Quaddakersd. W. J (2001). Oxide scale growth on MCrAlY bond coatings after pulsed electron beam treatment and deposition of EBPVD-TBC. *Surface and Coatings Technology*. 135 (2-3), 196-201.
52. Toscano. J, Vaben. R, Gil. A., Subanovic. M, Naumenko. D, Singheiser. L, (2006). Parameters affecting TGO growth and adherence on MCrAlY-bond coats for TBC's. *Surface and Coatings Technology*. 201(7) 3906–3910.
53. Choi. H, Yoon. B, Kim. H, Lee. C (2002). Isothermal oxidation of air plasma spray NiCrAlY bond coatings. *Surface and Coatings Technology*. 150 (2-3), 297–308.
54. Evans. A. G, Mumm. D. R, J. Hutchinson. W, Meier. G. H, Pettit. F. S (2001). Mechanisms controlling the durability of thermal barrier coating. *Progress in Materials Science*. 46 (5), 505-553.

55. Fan. X. L, Xu. R, Zhang. W. X, Wang. T.J (2012). Effect of periodic surface cracks on the interfacial fracture of thermal barrier coating system. *Applied Surface Science*. 258 (24), 9816–9823.
56. Wang. B, Gong. J, Sun. C, Huang. R.F, Wen. L.S (2003). The behavior of MCrAlY coatings on Ni₃Al-base superalloy. *Materials Science and Engineering A*. 357 (1-2), 39-44.
57. Khor. K. A, Gu. Y. W. (2000). Thermal properties of plasma-sprayed functionally graded thermal barrier coatings. *Thin Solid Films*. 372 (1-2), 104-113.
58. Shilington. E. A. G, Clarke. D. R (1999). Spalling failure of a thermal barrier coating associated with aluminum depletion in the bond-coat. *Acta Materialia*. 47 (4), 1297-1305.
59. Zhou. Z, Guo. H, Wang. J, Abbas. M, Gong. S (2011). Microstructure of oxides in thermal barrier coatings grown under dry/humid atmosphere. *Corrosion Science*, 53 (8), 2630-2635.
60. Zhou. C, Wang. N, Xu. H (2007). Comparison of thermal cycling behavior of plasma-sprayed nanostructured and traditional thermal barrier coatings. *Materials Science and Engineering A*. 452–453, 569–574.
61. Stiger. M. J, Yanar. N. M, Pettit. F.S, Meier. G. H, Hampikian. J. M, N. B. Dahotre (1999). Elevated Temperature Coatings: *Science and Technology III, The minerals. Metals & Materials Society*. San Diego, CA, 122-130.
62. Ren. C, He. Y.D, Wang. D. R (2011). Preparation and characteristics of three-layer YSZ–(YSZ/Al₂O₃)–YSZ TBCs. *Applied Surface Science*. 257(15), 6837–6842.
63. Marginean. G, Utu. D (2012). Cyclic oxidation behavior of different treated CoNiCrAlY coatings. *Applied Surface Science*. 258(20), 8307–8311.
64. Takahashi. S, Yoshiba. M, Harada. Y (2003). Nano-Characterization of Ceramic Top-Coat/Metallic Bond-Coat Interface for Thermal Barrier Coating Systems by Plasma Spraying. *Materials Transactions*. 44 (6), 1181 – 1189.
65. Hille. T. S, Suiker. A. S (2009). Micro-crack nucleation in thermal barrier coating systems. *Engineering Fracture Mechanics*. 76 (6), 813–825.
66. Richer. P, Yandouzi. M, Beauvais. L, Jodoin. B (2010). Oxidation behavior of CoNiCrAlY bond coats produced by plasma, HVOF and cold gas dynamic spraying. *Surface and Coatings Technology*. 204 (24), 3962–3974.

67. Keyvani. A, Saremi. M, Heydarzadeh Sohi. M (2011). Oxidation resistance of YSZ-alumina composites compared to normal YSZ TBC coatings at 1100°C. *Alloys and compounds*. 509 (33), 8370-8377.
68. Picas. J. A, Forn. A, Ajdelsztajn. L, Schoenung. J (2004). Nanocrystalline NiCrAlY powder synthesis by mechanical cryomilling. *Powder Technology*. 148 (1), 20-23.
69. Suryanarayana. C (2001). Mechanical alloying and milling. *Progress in Materials Science*. 46 (1-2), 1-184.
70. LIU. C. b, ZHANG. Z. M, JIANG. X. I, LIU. M, ZHU. Z. h (2009). Comparison of thermal shock behaviors between plasma-sprayed nanostructured and conventional zirconia thermal barrier coatings. *Transactions of Nonferrous Metals Society of China*. 19 (1), 99-107.
71. Baia. Y, Hana. Z.H, Li. H.Q, Xua. C, Xu. Y. L, Wang. Z, Ding. C. H, Yang. J. F (2011). High performance nanostructured ZrO₂ based thermal barrier coatings deposited by high efficiency supersonic plasma spraying. *Applied Surface Science*. 257 (16), 7210–7216.
72. Wang. N, Zhou. C, Gong. S, Xu. H (2007). Heat treatment of nanostructured thermal barrier coating. *Ceramics International*. 33 (6), 1075–1081.
73. Wang. H, Zuo. D, Chen. G, Sun. G, Li. X, Cheng. X (2010). Hot corrosion behavior of low Al NiCoCrAlY clad coatings reinforced by nano-particles on a Ni-base super alloy. *Corrosion Science*. 52 (10), 3561-3567.
74. Hong. Z, Bo. H, Jun. W, Bao. S (2007). Nanostructured yttria stabilized zirconia coatings deposited by air plasma spraying. *Transactions of Nonferrous Metals Society of China*. 17 (2), 389-393.
75. Zeng. Yi, Lee. S. W, Gao. L (2002). Atmospheric plasma sprayed coatings of nanostructured zirconia. *European Ceramic Society*. 22 (3), 347–351.
76. Xu. Z, He. L, Mu. R, He. S, Huang. G, Cao. X (2010). Hot corrosion behavior of rare earth zirconates and yttria partially stabilized zirconia thermal barrier coatings. *Surface and Coatings Technology*. 204 (21-22), 3652 - 3661.
77. Zhong. X. H, Wang. Y. M, Xu. Z. H, Zhang. Y. F, Zhang. J. F, Cao. X. Q (2010). Hot-corrosion behaviors of overlay-clad yttria-stabilized zirconia coatings in contact with vanadate sulfate salts. *European Ceramic Society*. 30 (6), 1401- 1408.

78. Ramachandra. C, Lee. K. N, Tewari. S. N (2003). Durability of TBCs with a surface environmental barrier layer under thermal cycling in air and in molten salt. *Surface and Coatings Technology*. 172 (2-3), 150–157.
79. Habibi. M. H, Wang. Li, Guo. S. M. (2012). Evolution of hot corrosion resistance of YSZ, $Gd_2Zr_2O_7$, and $Gd_2Zr_2O_7 + YSZ$ composite thermal barrier coatings in $Na_2SO_4 + V_2O_5$ at 1050 °C. *European Ceramic Society*. 32 (8), 1635–1642.
80. Munz. D, Fett. T (1999). Mechanical properties, Failure behavior. *Materials selection*. Berlin, Springer. 9 (10), 135.
81. Wu. Y. N, Ke. P. L, Wang. Q. M, Sun. C, Wang. F.H (2004). High temperature properties of thermal barrier coatings obtained by detonation spraying. *Corrosion Science*. 46 (12), 2925–2935.
82. Shaw. L. L, Goberman. D, Ren. R, Gell. M, Jiang. S, Wang. Y, Xiao. T. D, Strutt. P. R (2000). The dependency of microstructure and properties of nanostructured coatings on plasma spray conditions. *Surface and Coatings Technology*. 130 (1), 1-8.
83. Qiana. Y, Dua. b. L, Zhanga. W (2009). Preparation of Spherical Y_2SiO_5 Powders For Thermal-Spray Coating. *Particuology*. 7 (5), 368–372.
84. Garcia. E, Mesquita. J, Miranzo. P, Osendi. M. I, Wang. Y, Lima. R. S, Moreau. N (2009). Mullite and Mullite/ ZrO_2 -7wt.% Y_2O_3 Powders for Thermal Spraying of Environmental Barrier Coatings. *Thermal Spray technology*. 19 (1-2), 286–293.
85. Markinauskas. L (2010). Deposition of Alumina Coatings from Nanopowders by Plasma Spraying. *Journal of Materials Science (MEDŽIAGOTYRA)*. 16 (1), 47-51.
86. Lima. R. S, Marple. B. R (2007). Thermal Spray Coatings Engineered from Nanostructured Ceramic Agglomerated Powders for Structural, Thermal Barrier and Biomedical Applications: A Review. *Thermal Spray Technology*. 16 (1), 40-63.
87. Lin. X, Zeng. Y, Lee. S. W, Ding. C (2004). Characterization of alumina–3 wt.% titania coating prepared by plasma spraying of nanostructured powders. *European Ceramic Society*. 24 (4), 627–634.
88. Pidani. R. A, Razavi. R. S, Mozafarinia. R, Jamali. H (2012). Evaluation of hot corrosion behavior of plasma sprayed ceria and yttria stabilized zirconia

- thermal barrier coatings in the presence of $\text{Na}_2\text{SO}_4+\text{V}_2\text{O}_5$ molten salt. *Ceramics International*. 38(8), 6613–6620.
89. Tsai. P.C, Lee. J. H, Hsu. C. S (2007). Hot corrosion behavior of laser-glazed plasma-sprayed yttria-stabilized zirconia thermal barrier coatings in the presence of V_2O_5 . *Surface and Coatings Technology*. 201(9-11), 5143–5147.
 90. Nicholls. J. R, Lawson. K. J, Johnstone. A, Rickerby. D. S (2006). Methods to reduce the thermal conductivity of EB-PVD TBCs. *Surface and Coatings Technology*. 151 –152, 383–391.
 91. Sharafat. S, Kobayashi. A, Ogden. V, Ghoniem. N. M (2000). Development of composite thermal barrier coatings with anisotropic microstructure. *Vacuum*. 59 (1), 185-193.
 92. Kulkarni. A, Vaidya. A, Goland. A, Sampath. S (2003). Processing effects on porosity-property correlations in plasma sprayed yttria-stabilized zirconia coatings. *Materials Science and Engineering A*. 359 (1-2), 100-111.
 93. Rhys-Jones. T. N (1990). The use of thermally sprayed coatings for compressor and turbine applications in aero engines. *Surface and Coatings Technology*. 42(1), 1–11.
 94. Ng. H. W, Gan. Z (2005). A finite element analysis technique for predicting as-sprayed residual stresses generated by the plasma spray coating process. *Finite Elements in Analysis and Design*. 41 (13), 1235–1254.
 95. Nicholls. J. R, Deakin. M. J, Rickerby. D. S (1999). A comparison between the erosion behavior of thermal spray and electron beam physical vapor deposition thermal barrier coatings. *Wear*. 233–235, 352–361.
 96. Antoua. G, Montavonb. G, Hlawkaa. F. O, Corneta. A, Coddetb. C, Machi. F (2004). Evaluation of modifications induced on pore network and structure of partially stabilized zirconia manufactured by hybrid plasma spray process. *Surface and Coatings Technology*. 180 –181, 627–632.
 97. Ouyang. H, Sasaki. S (2002). Microstructural and tribological characteristics of $\text{ZrO}_2\text{-Y}_2\text{O}_3$ ceramic deposited by laser assisted plasma hybrid spraying. *Tribology International*. 35, 255-264.
 98. Lay. L. A (1991). *Corrosion resistance of technical ceramics*. Second edition, London, HMSO. 83.
 99. Richerson. D. W (1982). *Modern Ceramic engineering: properties, processing, and use in design*. New York, Marcel Dekker. 37, 72 and 134.

100. Kingery. W. D (1976). *Introduction to ceramics*. 2nd edition. Wiley Interscience, New York.
101. Courtright. E. L (1994). A review of fundamental coating issues for high temperature compositions. *Surface and coatings Technology*. 68-69, 116-125.
102. Andritschky. M, Cunha. I, Alpuim. P (1997). Thermal stability of zirconia/alumina thin coatings produced by magnetron sputtering. *Surface and coatings Technology*. 94-95, 144-148.
103. Voort. G. F. V (2004). *Metallography and Microstructures of Heat-Resistant Alloys*. ASM Handbook: Metallography and Microstructures. 9, 820–859.
104. Mobarra. R, Jafari. A. H (2006). Hot corrosion behavior of MCrAlY coatings on IN738LC. *Surface and Coatings Technology*. 201 (6), 2202–2207.
105. Sulzer Metco (2012). *Nickel Chromium Aluminum Yttrium (NiCrAlY) Thermal Spray Powders*. www.sulzer.com/.../DSMTS_0102_0_NiCrAlY.pdf-Switzerland.
106. Sulzer Metco (2012). *8% Yttria Stabilized Zirconia Agglomerated and HOSP Thermal Spray Powders*. [www.sulzer.com/.../DSMTS_0001_2_8YOZrO_HOSP .pdf-Switzerland](http://www.sulzer.com/.../DSMTS_0001_2_8YOZrO_HOSP.pdf-Switzerland).
107. Bradford. S. A (2001). *Corrosion Control*. (2th Edition). Canada. CASTI Publishing (ISBN 1-894038-58-4). Chapter 10, 328-329.
108. Takeuchi. S, ITO. M, Takeda. K (1990). Modeling of residual stress in plasma sprayed coatings: effect of substrate temperature. *Surface and coatings Technology*. 43-44 (part 1), 426-435.
109. Hashmi. M. S. J, Pappalettere. C, Ventola. F (1998). Residual stresses in structures coated by a high velocity oxy-fuel technique. *Journal of Materials Processing Technology*. 75 (1-3), 81-86.
110. Ajdelsztajn. L, Picas. J. A, Kim. G. E, Bastian. F. L, Schoenung. J, Provenzano. V (2002). Oxidation behavior of HVOF sprayed nanocrystalline NiCrAlY powder. *Materials Science and Engineering A*. 338 (1-2), 33–43.
111. Bolelli. G, Cannillo. V, Lusvardi. L (2006). Glass –Alumina composite coatings by plasma spraying, part 1: Microstructural and mechanical characterization. *Surface and Coatings Technology*. 201(1-2), 458-473.
112. Schlichting K. W, Padture. N. P, Jordan. E. Gell. H. M (2003). Failure modes in plasma-sprayed thermal barrier coatings. *Materials Science and Engineering A*. 342 (1-2), 120-130.

113. Seo, D, Ogawa, K (2012). Isothermal Oxidation Behavior of Plasma Sprayed MCrAlY Coatings. *Advanced Plasma Spray Applications*. In Tech.
114. Birk, N, Meier, G. H, Petit, F. S (1994). Forming continuous alumina scales to protect superalloys. *Oxidation of Metals*. 46 (12), 42-46.
115. Brandon, J. R, Taylor, R (1991). Phase stability of zirconia-based thermal barrier coatings part II. Zirconia-ceria alloys. *Surface and Coatings Technology*. 46 (1), 91-101.
116. Jones, R. L (1997). Some aspects of the hot corrosion of thermal barrier coatings. *Thermal Spray Technology*. 6 (1), 77-84.
117. Wu, N, Chen, Z, Mao, S. X (2005). Hot Corrosion Mechanism of Composite Alumina/Yttria-Stabilized Zirconia Coating in Molten Sulfate–Vanadate Salt. *American Ceramic Society*. 88 (3), 675–682.
118. Chen Z, Yuan, F, Wang, Z, Zhu, S (2007). The oxide scale formation and evaluation on detonation gun sprayed NiCrAlY coatings during isothermal oxidation. *Materials Transactions*. 48 (10), 2695-2702.
119. Chen, X, Zhao, Y, Gu, L. B, Zou, N, Wang, Y, Cao, X (2011). Hot corrosion behavior of plasma sprayed YSZ/LaMgAl₁₁O₁₉ composite coatings in molten sulfate–vanadate salt. *Corrosion Science*. 53 (6), 2335–2343.
120. Li, S, Liu, Z. G, Ouyang, J. H (2010). Hot corrosion behavior of Yb₂Zr₂O₇ ceramic coated with V₂O₅ at temperatures of 600–800°C in air. *Corrosion Science*. 52 (10), 3568-3572.
121. Nusair Khan, A, Lu, J (2003). Behavior of air plasma sprayed thermal barrier coatings, subject to intense thermal cycling. *Surface and Coatings Technology*. 166 (1), 37–43.
122. Jamali, H, Mozafarinia, R, Razavi, R. S, Ahmadi-Pidani, R (2012). Comparison of thermal shock resistances of plasma-sprayed nanostructured and conventional yttria stabilized zirconia thermal barrier coatings. *Ceramics International*. 38 (8), 6705-6712.